Paper 146

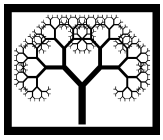

Proceedings of the Eleventh International Conference on Computational Structures Technology, B.H.V. Topping, (Editor), Civil-Comp Press, Stirlingshire, Scotland

Numerical Analysis of Thermo-Mechanical Wear Problems for Reciprocal Punch Sliding

I. Páczelt[1] and Z. Mróz[2]
[1]University of Miskolc, Hungary
[2]Institute of Fundamental Technological Research, Warsaw, Poland

Abstract

The relative sliding motion of two elastic bodies in contact induces wear process and contact shape evolution. The transient process tends to a steady state occuring at fixed contact stress and strain distribution. This state corresponds to the minimum of the wear dissipation power. The optimality conditions of the functional provide the contact stress distribution and the wear rate compatible with the rigid body punch motion. The present paper extends the previous analyses [1-5] of the steady state conditions to cases of periodic sliding of contacting bodies, assuming cyclic steady state conditions for both mechanical and thermal fields.

Keywords: contact problems, sliding wear, heat generation, steady-state, periodic sliding, optimal contact surface, *p*-version of finite elements.

1 Introduction

The present paper extends the previously published analyses of steady-state wear processes for monotonic sliding and fixed loading conditions of two contacting bodies B_1 and B_2, cf. Páczelt and Mróz [1-5] to the case of periodic sliding of contacting bodies, assuming cyclic steady state conditions with account for the heat generation at the contact surface.

For cases of monotonic sliding motion the minimization of the wear dissipation power provided the contact pressure distribution and rigid body wear velocities directly without time integration of the wear rule until the steady state is reached, cf. [1-5]. In the case of periodic sliding motion, the steady state cyclic solution should be specified and the averaged pressure in one cycle and the averaged wear velocity can be determined from the averaged wear dissipation in one cycle.

For reciprocal punch motion the steady state contact profile and pressure can be determined from steady state solutions for monotonic sliding. The first specific case is related to wear analysis induced by a punch periodically translating on an elastic

strip. Referring to the steady state contact pressure distributions for arbitrarily constrained punch and noting that the pressure at one contact edge vanishes, then the maximal pressure at the other edge is twice the mean pressure [6]. The analysis of the same example with heat generation demonstrates that the thermal distortion affects essentially the optimal contact shape, and also the distribution of contact pressure.

The numerical analysis of oscillating contact sliding motion without heat generation by Peigney [7], Kim et al [8], McColl et al. [9] and analytical treatment by Goryacheva et al. [10] demonstrate the existence of steady cyclic states attained in the wear process. The present numerical analysis will also demonstrate that for the case of heat generation during the periodic sliding motion the cyclic steady state wear process occurs with periodically varying mechanical and thermal fields.
In our analysis it is supposed that the gross slip (or sliding) regime develops between the contacting bodies In this case the sticking zone no longer exists and the whole contact zone undergoes sliding. The tangential contact traction can then be directly calculated from the contact pressure and the coefficient of friction.

1.1 Wear rule and wear rate vector

The modified Archard wear rule [1] specifies the wear rate $\dot{w}_{i,n}$ of the *i*-th body in the normal contact direction. Following the previous work [1, 3] it is assumed that

$$\dot{w}_{i,n} = \beta_i (\tau_n)^{b_i} \left\| \dot{\boldsymbol{u}}_\tau \right\|^{a_i} = \beta_i (\mu\, p_n)^{b_i} \left\| \dot{\boldsymbol{u}}_\tau \right\|^{a_i} = \quad \beta_i (\mu\, p_n)^{b_i} v_r^{a_i} = \widetilde{\beta}_i p_n^{b_i} v_r^{a_i}, \quad i = 1,2 \qquad (1)$$

where μ is the friction coefficient, β_i, a_i, b_i are the wear parameters, $\widetilde{\beta}_i = \beta_i \mu^{b_i}$, $v_r = \left\| \dot{\boldsymbol{u}}_\tau \right\|$ is the relative velocity which is given from rigid body movement of the bodies, constrained by the boundary conditions. The shear stress at the contact surface is denoted by τ_n and calculated in terms of the contact pressure p_n by using the Coulomb friction law $\tau_n = \mu\, p_n$.

However, in general contact conditions the wear rate vector $\dot{\mathbf{w}}_i$ is not normal to the contact surface and results from the constraints imposed on the rigid body motion of punch B_1. Introducing the local reference triad $\mathbf{e}_{\tau_1}, \mathbf{e}_{\tau_2}, \mathbf{n}_c$ on the contact surface S_c, where $\mathbf{n}_c$ is the unit normal vector, directed into body B_2, $\mathbf{e}_{\tau_1}$ is the unit tangent vector coaxial with the sliding velocity and $\mathbf{e}_{\tau_2}$ is the transverse unit vector. This means that at each point of the contact surface, the local reference triad is given.

The fundamental property of steady wear states was assumed in [5,6] for *Class 2* problems (The contact surface S_c does not evolve in the wear process but rather it is prescribed. The rigid body wear velocity is compatible with the specified boundary conditions. The steady state condition is reached when the contact stress distribution is fixed in the moving contact domain.) , namely the coaxiality of the

total wear rate vector $\dot{\boldsymbol{w}} = \dot{\boldsymbol{w}}_2 - \dot{\boldsymbol{w}}_1$ and the rigid body wear velocity vector $\dot{\boldsymbol{w}}_R = \dot{\boldsymbol{\lambda}}_F + \dot{\boldsymbol{\lambda}}_M \times \Delta \boldsymbol{r}$ of the indenter B_1, thus

$$\dot{\boldsymbol{w}} = \dot{\boldsymbol{w}}_2 - \dot{\boldsymbol{w}}_1 = \dot{\boldsymbol{w}}_R = \dot{\boldsymbol{w}}_{2,R} - \dot{\boldsymbol{w}}_{1,R} = -\dot{w}_{1,R}\, \boldsymbol{e}_R + \dot{w}_{2,R}\, \boldsymbol{e}_R = \dot{w}_R\, \boldsymbol{e}_R \tag{2}$$

where

$$\boldsymbol{e}_R = \frac{\dot{\boldsymbol{\lambda}}_F + \dot{\boldsymbol{\lambda}}_M \times \Delta \boldsymbol{r}}{\left\| \dot{\boldsymbol{\lambda}}_F + \dot{\boldsymbol{\lambda}}_M \times \Delta \boldsymbol{r} \right\|} \tag{3}$$

is the unit vector and $\dot{w}_R = \left\| \dot{\boldsymbol{\lambda}}_F + \dot{\boldsymbol{\lambda}}_M \times \Delta \boldsymbol{r} \right\|$, the rigid body wear velocities are $\dot{\boldsymbol{\lambda}}_F, \dot{\boldsymbol{\lambda}}_M$. Referring to the Fig. 1, the normal and tangential wear rate components are

$$\dot{w}_n = \dot{w}_R \cos\chi\,,\ \dot{w}_\tau = \dot{w}_R \sin\chi = \dot{w}_n \tan\chi\,, \tag{4}$$

where χ is the angle between $\boldsymbol{n}_c$ and $\boldsymbol{e}_R$. The wear rate components in the tangential directions can be easily defined using the angles χ and χ_1 which are shown in Fig. 1. The steady state conformity condition requires that $b_1 = b_2$ in the wear rule (1). The coaxiality condition (2) is naturally expected as the elastic stress and strain states are fixed on S_c and the shape evolution rate due to wear follows the relative rigid body velocity.

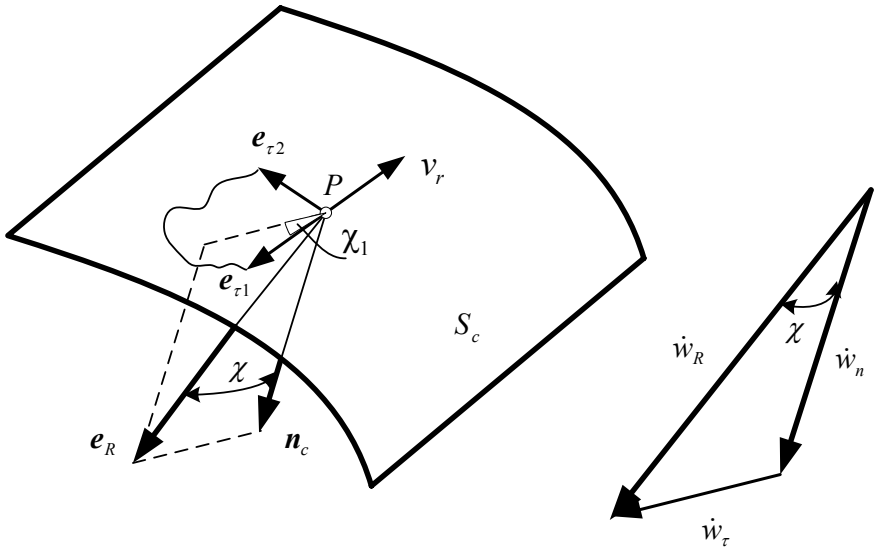

Figure. 1: Wear rate vectors on the contact surface S_c : coaxiality of $\dot{\boldsymbol{w}}_R$ and $\dot{\boldsymbol{w}}$.

The contact traction on S_c can be expressed as follows

$$\boldsymbol{t}^c = \boldsymbol{t}_1^c = -\boldsymbol{t}_2^c = -p_n \boldsymbol{\rho}_c^{\pm} \quad , \quad \boldsymbol{\rho}_c^{\pm} = \boldsymbol{n}_c \pm \mu \boldsymbol{e}_{\tau 1} - \mu_d \, \boldsymbol{e}_{\tau 2} \tag{5}$$

where $\boldsymbol{\rho}_c^{\pm}$ specifies the orientation and magnitude of traction $\boldsymbol{t}^c$ with reference to the contact pressure p_n and μ_d is the transverse friction coefficient. The sign + in (5) corresponds to the case when the relative velocity is $\dot{\boldsymbol{u}}_\tau = \dot{\boldsymbol{u}}_\tau^{(2)} - \dot{\boldsymbol{u}}_\tau^{(1)} = -\|\dot{\boldsymbol{u}}_\tau\| \boldsymbol{e}_{\tau 1} = -v_r \boldsymbol{e}_{\tau 1}$ with the corresponding shear stress acting on the body B_1 along $-\boldsymbol{e}_{\tau 1}$.

1.2 Steady state conditions for monotonic motion

The wear dissipation power for the case of wear of two bodies

$$D_w = \sum_{i=1}^{2} \left(\int_{S_c} (\boldsymbol{t}_i^c \cdot \dot{\boldsymbol{w}}_i) \; dS \right) = \sum_{i=1}^{2} C_i \quad , \tag{6}$$

The global equilibrium conditions for the body B_1 can be expressed as follows

$$\begin{aligned} \boldsymbol{f} &= -\int_{S_c} \boldsymbol{\rho}_c^{\pm} \; p_n \, dS + \boldsymbol{f}_0 = \boldsymbol{0} \\ \boldsymbol{m} &= -\int_{S_c} \Delta \boldsymbol{r} \times \boldsymbol{\rho}_c^{\pm} \; p_n \, dS + \boldsymbol{m}_0 = \boldsymbol{0} \end{aligned} \tag{7}$$

where $\boldsymbol{f}_0$ and $\boldsymbol{m}_0$ denote the resultant force and moment acting on the body B_1.

The contact pressure distribution resulting from the minimization procedure has the form, cf. [4]

$$p_n = \left(\frac{\dot{\boldsymbol{\lambda}}_F \cdot \boldsymbol{\rho}_c^{\pm} + \left(\dot{\boldsymbol{\lambda}}_M \times \Delta \boldsymbol{r} \right) \cdot \boldsymbol{\rho}_c^{\pm}}{K} \frac{1}{Q} \right)^{\frac{1}{b}} \tag{8}$$

where $K = \sum_{i=1}^{2} \widetilde{\beta}_i \, v_r^{a_i}$, $Q = 1 \mp \mu \tan\chi \cos\chi_1 - \mu_d \tan\chi \sin\chi$. This distribution does not depend on the elastic moduli of contacting bodies but depends on friction and wear parameters. The derived non-linear equations (7) and (8) can be solved by applying the Newton-Raphson technique or another nonlinear equation solver of a different mathematical program library. Introducing the values: $\widetilde{\dot{\boldsymbol{\lambda}}}_F = \frac{\dot{\boldsymbol{\lambda}}_F}{K}$, $\widetilde{\dot{\boldsymbol{\lambda}}}_M = \frac{\dot{\boldsymbol{\lambda}}_M}{K}$, it can be stated that $p_n = p_n(\widetilde{\dot{\boldsymbol{\lambda}}}_F, \widetilde{\dot{\boldsymbol{\lambda}}}_M)$ and the equilibrium equations $\boldsymbol{f}\left(\widetilde{\dot{\boldsymbol{\lambda}}}_F, \widetilde{\dot{\boldsymbol{\lambda}}}_M\right) = \boldsymbol{0}, \boldsymbol{m}\left(\widetilde{\dot{\boldsymbol{\lambda}}}_F, \widetilde{\dot{\boldsymbol{\lambda}}}_M\right) = \boldsymbol{0}$ depend only on $\widetilde{\dot{\boldsymbol{\lambda}}}_F, \widetilde{\dot{\boldsymbol{\lambda}}}_M$. In this way it is demonstrated, that the contact pressure distribution depends only on the transformed wear velocities $\widetilde{\dot{\boldsymbol{\lambda}}}_F, \widetilde{\dot{\boldsymbol{\lambda}}}_M$ and the coefficients μ, μ_d and *b*, that is the

pressure disdribution does not depend on the relative velocity v_r nor the wear parameters $\widetilde{\beta}_i, i = 1,2$.

1.3 Steady state conditions for periodic sliding motion

Consider now the contact problems for the case of periodic sliding motion, so that the relative displacement, stress and strain satisfies the conditions

$$u_\tau(t) = u_\tau(t + T_*), \quad \boldsymbol{\sigma}(t) = \boldsymbol{\sigma}(t + T_*), \quad \boldsymbol{\varepsilon}(t) = \boldsymbol{\varepsilon}(t + T_*) \tag{9}$$

where T_* is the period of sliding motion.

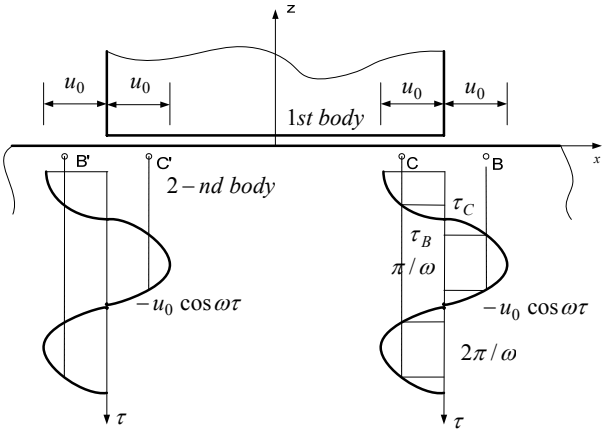

Figure 2: The wear process occurring at contact interface of a punch moving with the relative velocity $v_r = u_0\ \omega \sin\omega\tau$.

In particular, for the punch reciprocally sliding on the plane substrate along the linear path through the distance $s = 2u_0$ during each semi-cycle, the contact pressure varies periodically with the identical evolution during the rightward and leftward sliding at the symmetrical boundary conditions, thus $p_n(x) = p_n(s - x)$ and the shear stress is oriented in the opposite directions, that is $\tau_n(x) = -\tau_n(s - x)$. When wear of punch, or combined wear of punch and substrate occur, the progressive wear displacement at the contact will be fully controlled by the rigid body motion of one of contacting bodies, thus generating the continuing shape evolution preserving stress and strain periodicity.

Consider the periodic tangential relative displacement of body B_1 with respect to body B_2 in the direction $\boldsymbol{e}_{\tau 1}$

$$\boldsymbol{u}_\tau = -u_0 \cos\omega\tau\ \boldsymbol{e}_{\tau 1} \tag{10}$$

where u_0 and ω are the amplitude and angular velocity of the motion. The relative sliding velocity and the cycle period are

$$v_r = \left|\dot{\boldsymbol{u}}_\tau\right| = \left|\omega\, u_0 \sin\omega\tau\right| = \left|v_0 \sin\omega\tau\right|,\ T_* = \frac{2\pi}{\omega},\ v_0 = \omega u_0 \tag{11}$$

In the plane structure case the upper block (body B_1) is loaded by the force $\boldsymbol{F}_0 = -F_0\ \boldsymbol{e}_z$ with resulting moment M_0^y with respect to the y- axis. The Lagrangian multipliers $\dot{\lambda}_F$, $\dot{\lambda}_M^y$ represent the wear velocity components.

Let us define the wear dissipation in one cycle of sliding motion

$$E_w = \sum_{i=1}^{2} \int_0^{T_*} \left(\int_{S_c^{(i)}} (\boldsymbol{t}_i^c \cdot \dot{\boldsymbol{w}}_i)\, dS \right) d\tau = \sum_{i=1}^{2} \int_0^{T_*} \widetilde{C}_i\ d\tau \tag{12}$$

The functional (12) is to be minimized subject to constraints of equilibrium equations. For evaluation of (12) it is convenient to decompose the functional into two parts integrated over semi-cycles of progressive and reverse sliding, thus

$$E_w = \sum_{i=1}^{2} \int_0^{T_*/2} \left(\int_{S_c^{(i)}} (\boldsymbol{t}_i^{c+} \cdot \dot{\boldsymbol{w}}_i)\ \ dS \right) d\tau +$$

$$\sum_{i=1}^{2} \int_{T_*/2}^{T_*} \left(\int_{S_c^{(i)}} \boldsymbol{t}_i^{c-} \cdot \dot{\boldsymbol{w}}_i)\, dS \right)\ \ d\tau = \ \ \sum_{i=1}^{2} \int_0^{T_*/2} \left(\widetilde{C}_i^{+}\right)\ d\tau + \sum_{i=1}^{2} \int_{T_*/2}^{T_*} \left(\widetilde{C}_i^{-}\right) d\tau \tag{13}$$

The Lagrangian functional, that accounts for equilibrium conditions takes the form

$$L_{E_w} = L_{E_w}\left(p_n, \dot{\boldsymbol{\lambda}}_F, \dot{\boldsymbol{\lambda}}_M\right) = E_w\left(p_n\right) + (b+1) \int_0^{T_*} (\ \dot{\boldsymbol{\lambda}}_F \cdot \boldsymbol{f} + \dot{\boldsymbol{\lambda}}_M\ \cdot \boldsymbol{m})\, d\tau \tag{14}$$

Satisfying the stationary condition of (14), the contact pressure distribution has the following form for the case of wear of body B_1 (then $\widetilde{\beta}_2 = 0$, in rule (1))

$$p_n^{\pm} = \left(\frac{\dot{\boldsymbol{\lambda}}_F^{\pm} \cdot \boldsymbol{\rho}_c^{\pm} + \left(\dot{\boldsymbol{\lambda}}_M^{\pm} \times \Delta \boldsymbol{r}\right) \cdot \boldsymbol{\rho}_c^{\pm}}{\left[\ \left(\widetilde{\beta}_1\, v_r^{a_1}\right)\ \right]} (1 \mp \mu \tan\chi)^{-1} \right)^{\frac{1}{b}} \tag{15}$$

where the upper indices + or – in $\pm$ or $\mp$ sign apply respectively to first and second semi-cycles of progressive and reverse sliding.

Note that (15) specifies different pressure distributions for progressive and reverse sliding semi-cycles.

$$p_n^{\pm} = \left(\frac{\widetilde{\dot{\boldsymbol{\lambda}}}_F^{\pm} \cdot \boldsymbol{\rho}_c^{\pm} + \left(\widetilde{\dot{\boldsymbol{\lambda}}}_M^{\pm} \times \Delta \boldsymbol{r}\right) \cdot \boldsymbol{\rho}_c^{\pm}}{1 \mp \mu \tan\chi}\ \right)^{\frac{1}{b}} = p_n^{\pm}(\widetilde{\dot{\boldsymbol{\lambda}}}_F, \widetilde{\dot{\boldsymbol{\lambda}}}_M) \tag{16}$$

where

$$\widetilde{\dot{\boldsymbol{\lambda}}}^{\pm}_{F,M} = \frac{\dot{\boldsymbol{\lambda}}^{\pm}_{F,M}}{\widetilde{\beta}_1 v_r^{a_1}}. \tag{17}$$

Using the equilibrium equations for body 1 after substituting contact pressure

$$\begin{aligned} \boldsymbol{f} &= -\int_{S_c} \boldsymbol{\rho}_c^{\pm}\, p_n^{\pm}\, dS + \boldsymbol{f}_0 = \boldsymbol{0} \\ \boldsymbol{m} &= -\int_{S_c} \Delta \boldsymbol{r} \times \boldsymbol{\rho}_c^{\pm}\, p_n^{\pm}\, dS + \boldsymbol{m}_0 = \boldsymbol{0} \end{aligned} \tag{18}$$

it is easy to write that

$$\boldsymbol{f} = \boldsymbol{f}\,(\widetilde{\dot{\boldsymbol{\lambda}}}^{\pm}_{F}, \widetilde{\dot{\boldsymbol{\lambda}}}^{\pm}_{M}) = \boldsymbol{0}, \quad \boldsymbol{m} = \boldsymbol{m}\,(\widetilde{\dot{\boldsymbol{\lambda}}}^{\pm}_{F}, \widetilde{\dot{\boldsymbol{\lambda}}}^{\pm}_{M}) = \boldsymbol{0}, \tag{19}$$

that is the contact pressure is independent of the value of relative velocity v_r and wear parameter $\widetilde{\beta}_1$, but it is dependent on the sliding direction.

The Lagrangian vectors $\dot{\boldsymbol{\lambda}}_F, \dot{\boldsymbol{\lambda}}_M$ specifying the wear velocities of body B_1 can be calculated from the equilibrium equations (18) by applying Newton-Raphson technique. The case of wear of two bodies is similarly treated.

Let us define the average value of the relative velocity and the rigid body wear velocity vector in the one periodic motion

$$\overline{v}_r = \frac{1}{T_*}\int_0^{T_*} v_0 \left|\sin \omega\tau\right| d\tau\,, \quad \overline{\dot{\boldsymbol{\lambda}}}_{F,M} = \frac{1}{T_*}\int_0^{T_*} \dot{\boldsymbol{\lambda}}_{F,M}\, d\tau \tag{20}$$

It is easy to calculate the average normal wear rate for body 1 (provided body 1 is allowed to translate in the vertical direction)

$$\overline{\dot{w}}^{\pm}_{1,n} = \widetilde{\beta}_1 \left(\overline{p}_n^{\pm}\right)^b \overline{v}_r^{a_1} = \overline{\dot{\lambda}}^{\pm}_F = const\, 2 \tag{21}$$

and the average contact pressure equals

$$\overline{p}_n^{+} = \frac{2}{T_*}\int_0^{T_*/2} p_n^{+} d\tau = p_n^{+}, \; \overline{p}_n^{-} = \frac{2}{T_*}\int_{T_*/2}^{T_*} p_n^{-} d\tau = p_n^{-} \tag{22}$$

1.4 Heat generation

Consider now the thermo-mechanical problem of wear with account for temperature effect. The temperature field can be generated by external heat sources and by the

frictional and wear dissipation at the contact interface. The friction dissipation power between the bodies generates the specific heat source

$$q_F = \tau_n \, v_r = \mu \, p_n \, v_r \tag{23}$$

which is split among debris and the contacting bodies 1 and 2, that is $q^d = \gamma^d \, q_{F,}$ $\hat{q}_F = q_F - q^d = \gamma^l \, q_F \quad \boldsymbol{x} \in S_c$, where $\gamma^l = 1 - \gamma^d$ and $0 < \gamma^d < 1$ are the heat partition coefficients for debris. By assuming perfect contact conditions, the temperature difference on the surfaces $S_c^{(1)}, S_c^{(2)}$ is neglected by some authors, cf. Komanduri and Hou [11], Zagrodzki [12], so one can write

$$\hat{q}_F^{(1)} + \hat{q}_F^{(2)} = \hat{q}_F \, , \; \theta^{(1)} = \theta^{(2)} \;\; \boldsymbol{x} \in S_c \tag{24}$$

Here $\theta^{(1)}, \theta^{(2)}$ are the temperatures on S_c of bodies 1 and 2. Calculation process of the thermo-mechanical-wear problem is described in detail in the paper [3, 4, 13, 14].

The average heat flux equals

$$\overline{q}_F^{+} = \frac{2}{T_*} \int_0^{T_*/2} q_F^{+} d\tau \, , \quad \overline{q}_F^{-} = \frac{2}{T_*} \int_{T_*/2}^{T_*} q_F^{-} d\tau \tag{25}$$

2 Examples

2.1 Numerical calculation of the wear and heat flux

In this section we analyse the wear process induced by the reciprocal punch translation Our goal is to specify the contact pressure distribution and the corresponding shape of contact surface in the steady wear state. It is assumed that only the punch will undergo wear. The wear parameters are: $\widetilde{\beta}_1 = 1.25\pi \cdot 10^{-8}, \widetilde{\beta}_2 = 0$, $a_1 = 1, b = 1$, the coefficient of friction is $\mu = 0.25$. The displacement of body 1 is: $u = -u_0 \cos \omega\tau$, where $u_0 = 1.5 \; mm$, $\omega = 10 \; rad/s$, τ is the time. During the one half period the wear is calculated in the following way

$$\Delta w_{1,n} = \widetilde{\beta}_1 \, p_n(t_p) \int_0^{T_*/2} u_0 \omega \left| \sin \omega\tau \right| d\tau \tag{26}$$

where t_p is the time of start of the half period. For simplified calculation the contact pressure $p_n = p_n(t_p)$ is assumed to be fixed during the half period. However, the pressure has different distributions during the left and rightward sliding directions.

The accumulated wear at the end of half period equals

$$w_{1,n} = w_{1,n}(t_p + T_*/2) = w_{1,n}(t_p) + \Delta w_{1,n} = w_{1,n}(t_p) + \widetilde{\beta}_1\, p_n(t_p)\, 2\, u_0 \tag{27}$$

Using the (25), (23), (11) the average heat flux on the contact boundary is

$$\begin{aligned} \overline{q}_F^{+} &= \frac{2}{T_*}\int_0^{T_*/2} q_F^{+} d\tau = \mu\, p_n^{+}(t_p)\,\frac{2u_0}{\pi}\,\omega\,, \\ \overline{q}_F^{-} &= \frac{2}{T_*}\int_0^{T_*/2} q_F^{-} d\tau = \mu\, p_n^{-}(t_p)\,\frac{2u_0}{\pi}\,\omega\,, \end{aligned} \tag{28}$$

that is the relative velocity for calculation of the monotonic motion is equal to $v_r = 2u_0\omega/\pi$ and the contact pressure is taken from solution of the minimization wear dissipation power problem, see. (6)-(8), or (14)-(19).

2.2 Example 1: sliding and rotating punch

The plane punch construction and boundary constraint are shown in Figure 3. The punch is allowed to translate in the normal direction and rotate around the pin support at O. The thickness of punch and strip is $t_{th} = 10\ mm$, the punch width is $L = 60\ mm$, its height is $h = 100\ mm$. The position height of the pin $l_z = 20\ mm$ or $l_z = 40\ mm$. The punch is loaded on the upper boundary $z = 200\ mm$ by the uniform pressure $p^{\sim} = 16.666\ MPa$ corresponding to the resultant vertical force $F_0 = 10.0\ kN$. The upper parts of the punch and strip are assumed to be made of the same materials, (Material 1, see Table 1). The lower punch portion of height 20 mm is characterized by the material parameters of Material 2, see Table 1.

Assume that relative velocity between the bodies for monotonic motion is $v_r = 200\ mm/s$. In this case, in the leftward direction the rigid body wear velocities are ($l_z = 20\,mm$): $\dot{\lambda}_F = 0.05\ mm/s,\ \dot{\lambda}_M = -5.55\times10^{-4}\ rad/s$ and for the rightward direction $\dot{\lambda}_F = 0.0166\ mm/s,\ \dot{\lambda}_M = 5.55\times10^{-4}\ rad/s$.
At $l_z = 40\,mm$ for the leftward direction of sliding velocity provides: $\dot{\lambda}_F = 0.06666\ mm/s,\ \dot{\lambda}_M = -0.001111\ rad/s$ and for the rightward sliding velocity: $\dot{\lambda}_F = 0.0\ mm/s,\ \dot{\lambda}_M = 0.001111\ rad/s$.

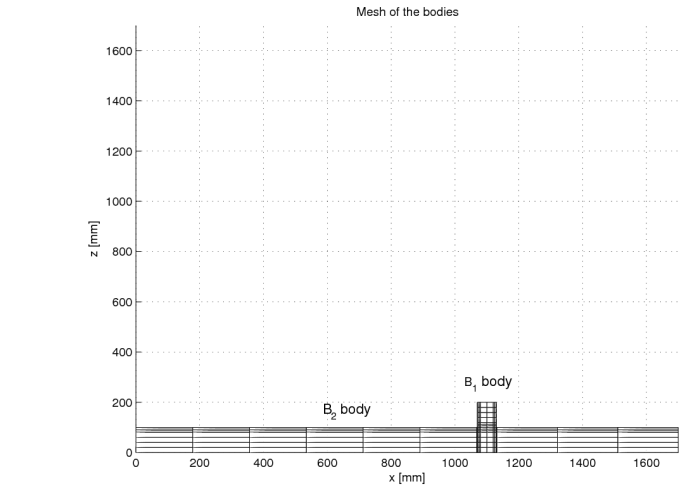

a)

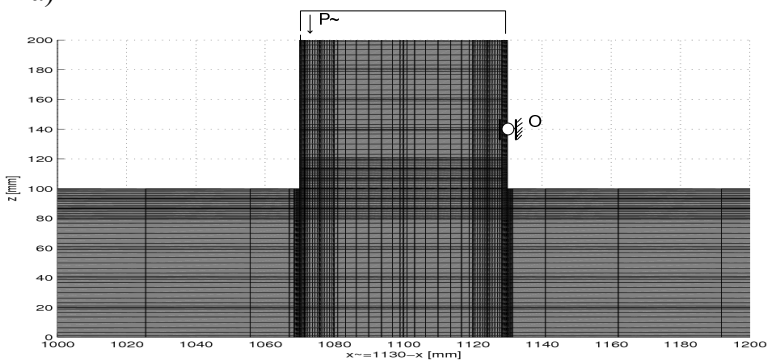

b)

Figure 3**:** The analysis of the wear process for the reciprocal sliding motion, a) the elastic punch B1, and the strip B2 translating in the leftward or rightward direction., b) mesh of body 1 (punch) and of central part of body 2 (strip). The horizontal and vertical lines correspond to Lobatto integration points. Number of elements at the contact zone in the *z*- direction is 8 and in the vertical *x* direction is 7 for both bodies. The finite elements are *p*-extension elements [15].

	Conductivity coeff. $K^{(i)}$ $[W/(m\,K)]$	Contact heat transfer- and the convection coefficient $\hat{h}_c, h_c^{(i)}$ $[W/(m^2\,K)]$	Heat capacity. $c^{(i)}$ $[J/(kgK)]$	Coeff. of thermal expansion $\alpha_\theta^{(i)}.10^5$ $[1/K]$	Young modul $E^{(i)}.10^{-5}$ $[MPa]$	Poisson ratio $\nu^{(i)}$	Material density $\rho^{(i)}$ $[kg/m^3]$
Material 1 (steel)	55	80	460	1	2	0.3	7800
Material 2 (composite)	5	80	1200	3	1.3	0.23	846

Table 1. Mechanical and thermal parameters of two materials

2.2.1 Wear analysis with neglect of heat generation

The numerical results of paper [6] are collected in Figures 4 and 5.

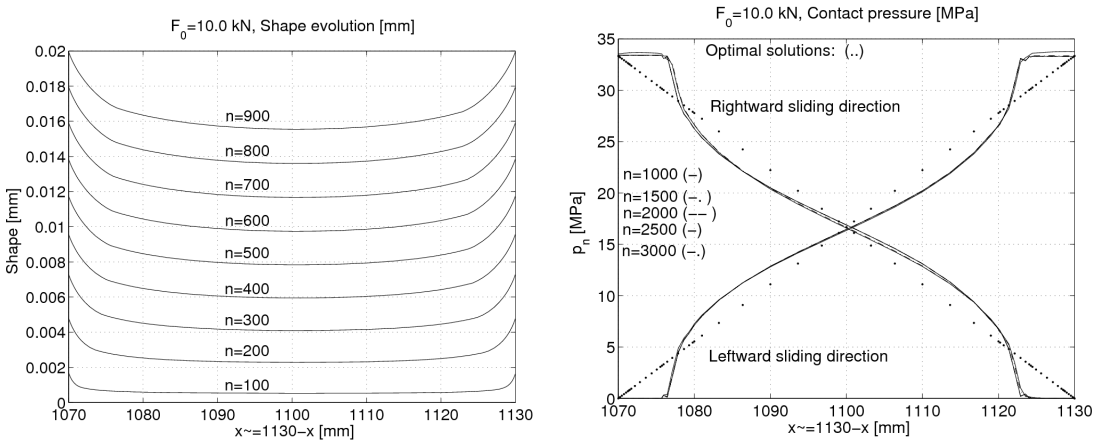

a) b)

Figure 4: a) Evolution of shape of Body 1 for reciprocal motion, b) Contact pressure at different time steps and sliding direction, $l_z = 40\,mm$.

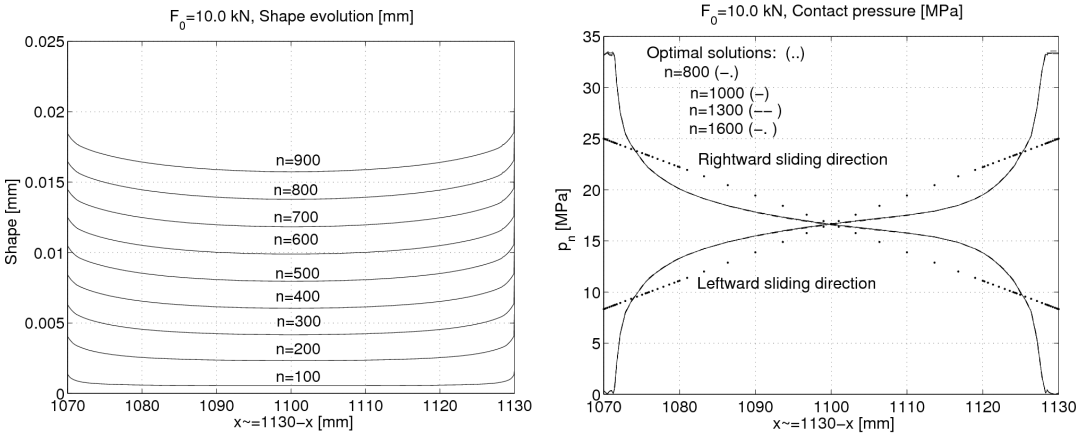

a) b)

Figure 5: a) Evolution of shape of Body 1 for reciprocal motion, b) Contact pressure at different time steps and sliding direction, $l_z = 20\,mm$.

The important conclusion can be drawn: for reciprocal punch motion the steady state contact profile and pressure can be determined from steady state solutions for monotonic sliding. Referring to the steady state contact pressure distributions in Figures 4 and 5 for non-symmetrically constrained punch and noting that the pressure at one contact edge vanishes, then the maximal pressure at the other edge is twice the mean (average of the optimal solutions) pressure. The same conclusion can also be stated for the symmetrically constrained punch, see Figure 9 in the example 2.

2.2.2 Wear analysis with account for heat generation

The stress and temperature fields are calculated in the iterative numerical process and the weak forms of equilibrium and heat conduction equations are applied [4,5]. The coupled thermo-mechanical problem is solved by the operator split technique. The mechanical and thermal fields discretized by the finite element approximation will be specified separately in the consecutive time steps. The wear effect is calculated incrementally by applying the wear rule (1).

The iterational process is organized in the following way.

At the beginning the half period motion the contact pressure and shape form are specified. At the end of the half period motion the contact pressure is fixed and by using the transient heat conduction a new value of temperature field is calculated. This generates small variation of contact geometrical conditions and of contact pressure distribution.

The pressure is predicted as follows

$$p_n^{(j)} = p_{n,s}\,(1-\gamma) + p_{n,s+1}^{(j)}\,\gamma\,,\ 0 \le \gamma \le 1,\quad j = 1,2,....,m\,. \tag{29}$$

This j type iterational process is repeated until the convergence criterion is satisfied, thus

$$e_w = 100\left|\int_{S_c}\left(g_s + w_{s+1}^{(j)}\right)dS - \int_{S_c}\left(g_s + w_{s+1}^{(j-1)}\right)dS\right| \Big/ \int_{S_c}\left(g_s + w_{s+1}^{(j-1)}\right)dS \le 0.01 = \tau_w \tag{30}$$

Here g_s is the initial gap at the beginning of the motion step $s+1$. After the convergence the reversal motion direction is considered, and the procedure follows the same steps.

For each motion direction step, the heat conduction problem is solved by using small time interval to reach the accurate value of the temperature field. In our case the half period time is devoted in 5 parts. Because the heat generation is different in the leftward and rightward moving direction, the acceleration of the calculation procedure of time integration of the wear rule is not possible. In this case, the method of extrapolation factor [5] is not used.

In Figures 6 and 7 the parameter $n = s$ is equal to double of the number of motion cycles.

2.2.1.1 Analysis of the case when the pin support height is $l_z = 40\,mm$

The heat conduction problem is solved for the following boundary conditions*:*

On the boundaries $z = 0, x = -\infty$ and $x = 1670\,mm$ the temperature is specified: $\theta_a = 0$, on the other parts of the boundary ($\boldsymbol{x} \in S_q^{(i)}, i = 1,2$) and over the domain of

bodies the heat flux is specified by the convection rule between the bodies and the surrounding medium. /these boundary conditions are valid for all examples/.

The shape evolution is defined by the time integration of the wear rule (1), calculated by (27). In the centre of contact zone the height of shape profile is larger than that at the boundary, see Figure 6a, the contact pressure is demonstrated at the different time step in Figure 6b.

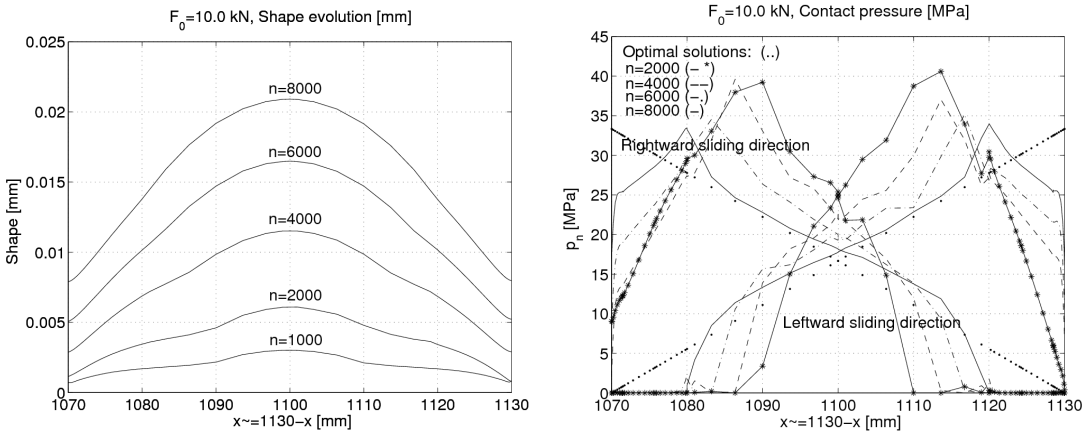

a) b)

Figure 6: a) Evolution of shape of Body 1 for reciprocal motion in the case of the heat generation, b) Contact pressure at different time steps and sliding directions, $l_z = 40\,mm$

2.2.2.2 The pin support height is $l_z = 20\,mm$

Using the same calculation technique, the evolution of the shape and contact pressure is demonstrated in Figures 7 a,b and 7 c-e. The temperature has larger value in the middle of punch, see Figures 8 a,b. The effect of wear it is evident, the temperature distortion is also larger in the middle part of the contact zone, that is the shape has a bell form. The contact pressure has different distribution form in the leftward and rightward sliding motion. The maximum value is increased and width of contact is decreased, but after $n = 1800$ the maximum value of pressure is reduced. Since the contact problems are solved without positioning technique [16], the pressure distribution function exhibits small oscillation around at the contact zone boundary points.

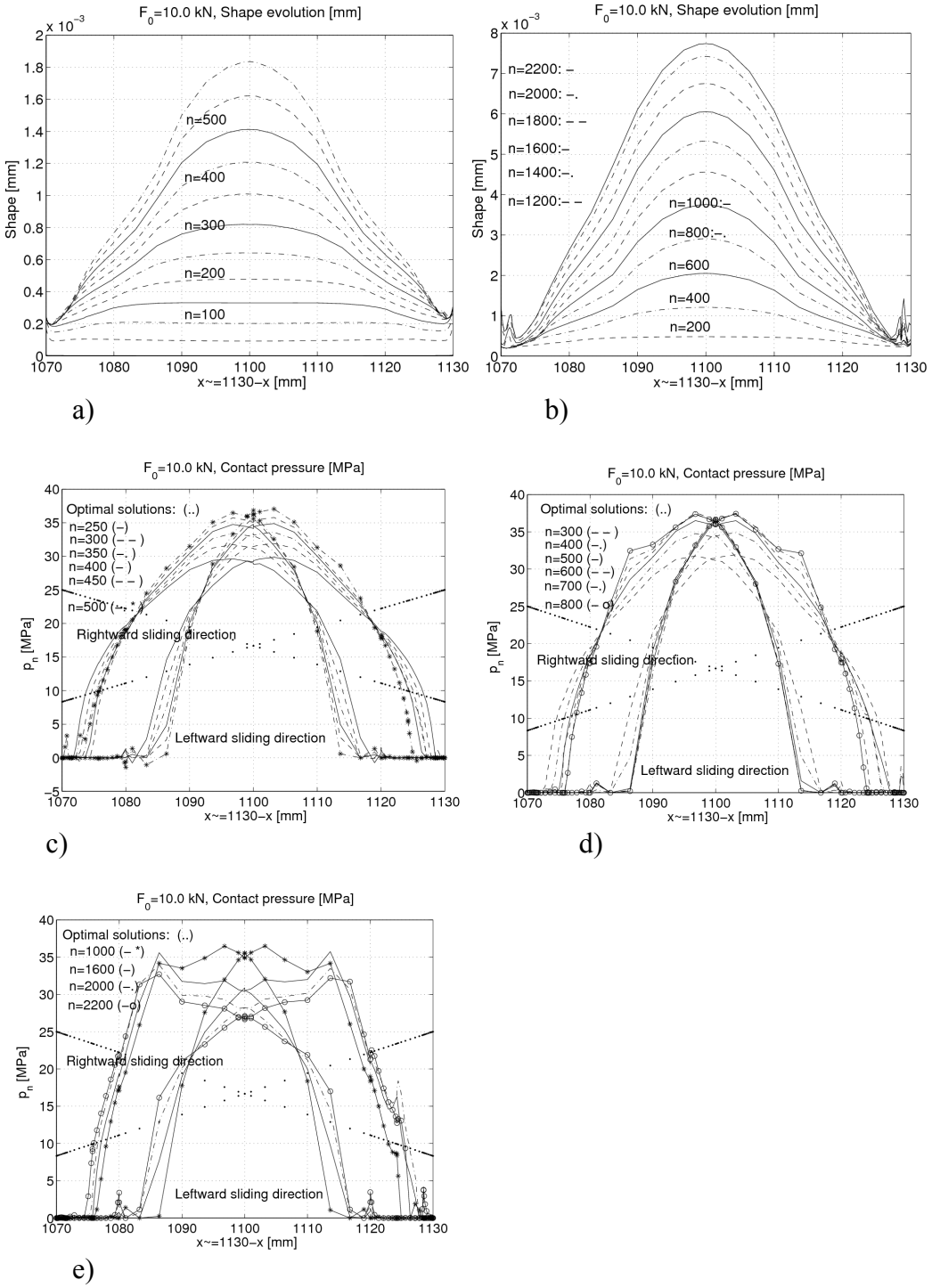

Figure 7: a,b) Evolution of shape of Body 1 for reciprocal motion in the case of the heat generation, c-e) Contact pressure at the different time steps and sliding directions, $l_z = 20\,mm$

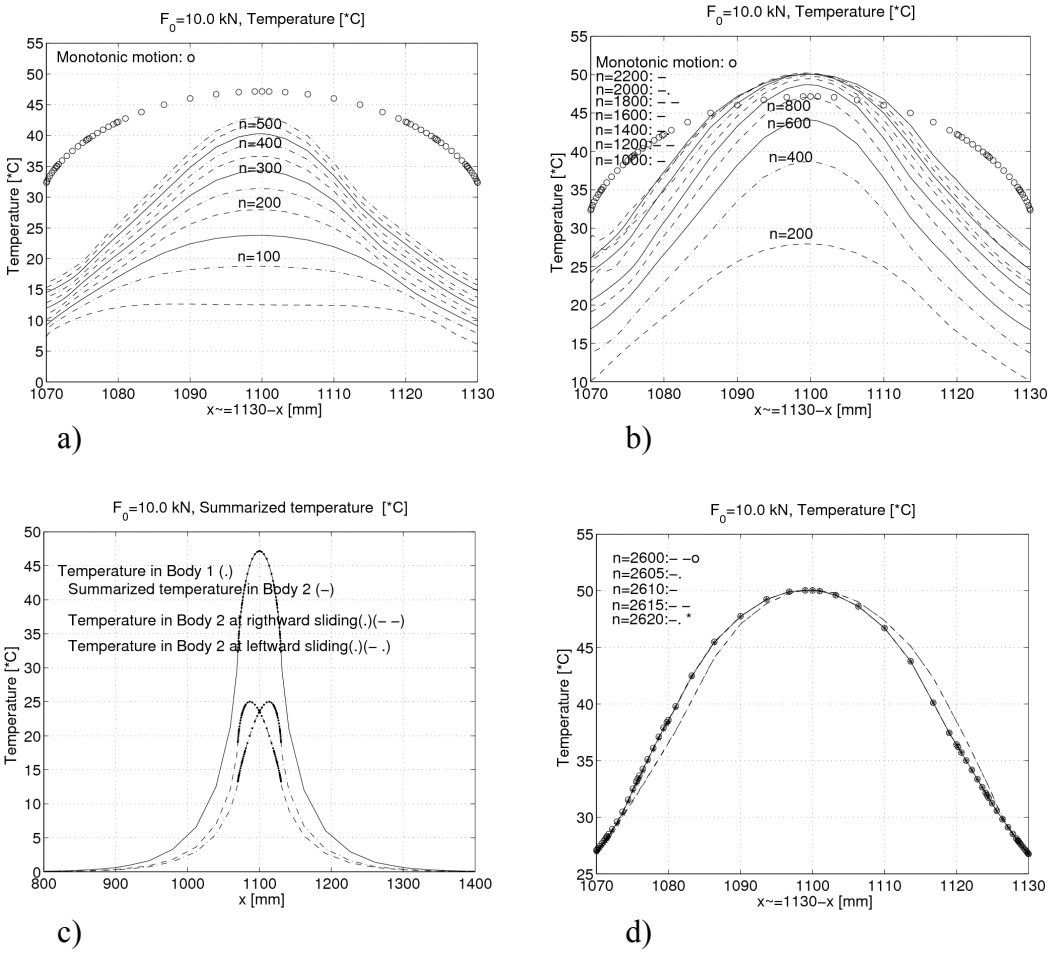

Figure 8: Temperature distribution on the contact boundary: a) , b) in the punch at different time steps for reciprocal motion, c) along the boundaries at $z = 100\,mm$ for monotonic motions, d) temperature at different time steps for periodic motion, for $n = 2600,2610,2620$ corresponds to leftward motion , for $n = 2605,2615$ to rightward motion direction.

The solution of heat conduction problem provides different temperature distribution for leftward and rightward monotonic sliding directions of the strip. Figure 8c demonstrates these temperatures, and the sum of these values on the contact boundary. This summed temperature /marked by (o)/ represents the temperature for reciprocal motion until $n = 800$, see Figure 8a,b, and temperature at $n \geq 800$ does not grow significantly over this curve. The maximum of the temperature very little varies after $n = 1400$. Since at the punch edges the contact pressure vanishes in the steady periodical wear state /see Figure 7c-e)/, the heat flux in these regions is also lower as compared to the monotonic case. The resultant average flux does not depend on the sliding direction

$$Q_F^+ = \int_{S_c} \overline{q}_F^+ \, dS = \int_{S_c} \mu \, p_n^+(t_p) \frac{2u_0}{\pi} \omega \, dS = \mu \, F_0 \frac{2u_0}{\pi} \omega = Q_F^- \tag{31}$$

The resulting temperature may now be taken as the sum of temperatures of opposite sliding directions, see Figure 8c. The maximum at the point $x = 1100\,mm$ is equal to $\theta_{\max}^{monotonic} = 47.16\ ^{o}C$. The relative error between the maximum temperature of periodic motion $\theta_{\max}^{periodic,n=2200} = 50.11\ ^{o}C$ and $\theta_{\max}^{monotonic}$ is:

$error_{\theta} = 100\,(\theta_{\max}^{periodic,n=2200} - \theta_{\max}^{monotonic}) / \theta_{\max}^{periodic,n=2200} = 5.89\%$. It can be stated that the maximum of temperature for the monotonic motion provides a good prediction of the maximum of temperature for the periodic motion.

At the large number of cycles *n* the temperature distributions are repeated for even and odd numbers of semicycles. We can therefore state that the wear process reached the periodical steady state, see Figure 8 d.

2.3 Example 2

Let us discuss the wear analysis for symmetrically distributed hinge supports of the punch, cf. Figure 9. The strip is assumed to perform reciprocal motion specified by the same parameters as in Example 2. The punch now is allowed to execute a rigid body vertical wear velocity $\dot{\lambda}_F$.

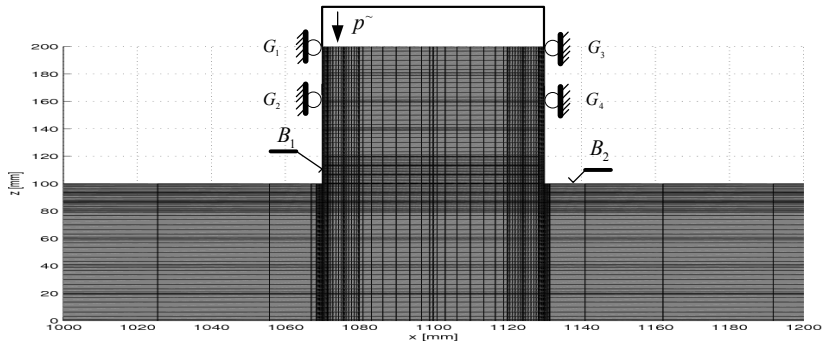

Figure 9. Mesh of body 1 (punch) and of central part of body 2 (strip), supports $G_i\ i = 1,4$

2.3.1 Wear analysis with neglect of heat generation

The summarized results taken from paper [6] are collected in Figure 10, presenting the contact shape evolution and distribution of the contact pressure at different time steps. In this case the contact pressure is also different for the leftward and rightward sliding motion. In the steady wear state the pressure maximum is two times greater than the average value (optimal solutions of the minimization problem (12)-(18)).

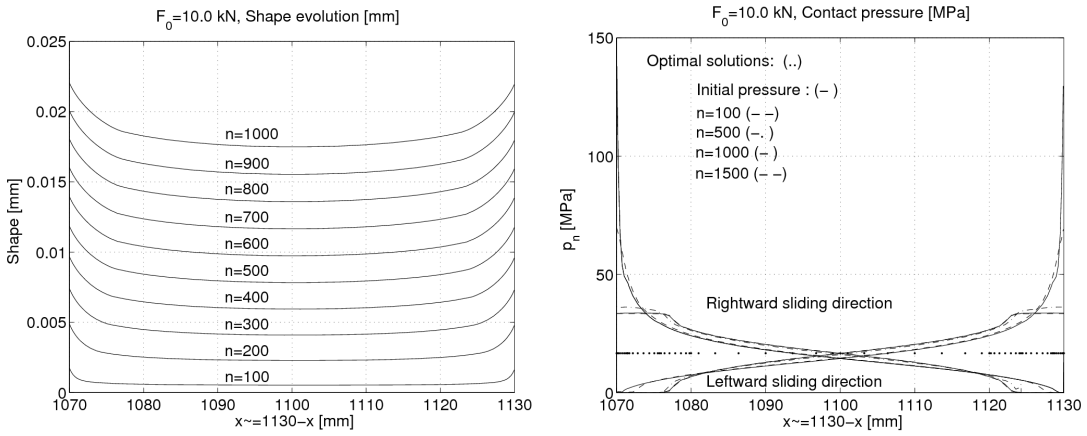

a) b)

Figure 10: a) Evolution of shape of Body 1 at periodic motion of substrate in Figure 8, b) contact pressure at different time steps and sliding directions.

2.3.2 Wear analysis with account for heat generation

In this case the rigid body wear velocity has only vertical component. The contact shape evolution and distribution of the contact pressure are presented at different time steps in the Figure 11, 12 a,b. The temperature has larger value in the middle of punch, see Figure 12 c. The periodic motion induces different contact pressure distribution during leftward and rightward directions. The contact pressure maximum therefore increases. In the case of the monotonic sliding motion the average pressure during the left a rightward sliding is constant, however, for the periodical motion it is not true, see Figure 13, at the centre there is $p_{n,\max}^{average} \approx 2 p_n^{opt} = 33.33\, MPa$.

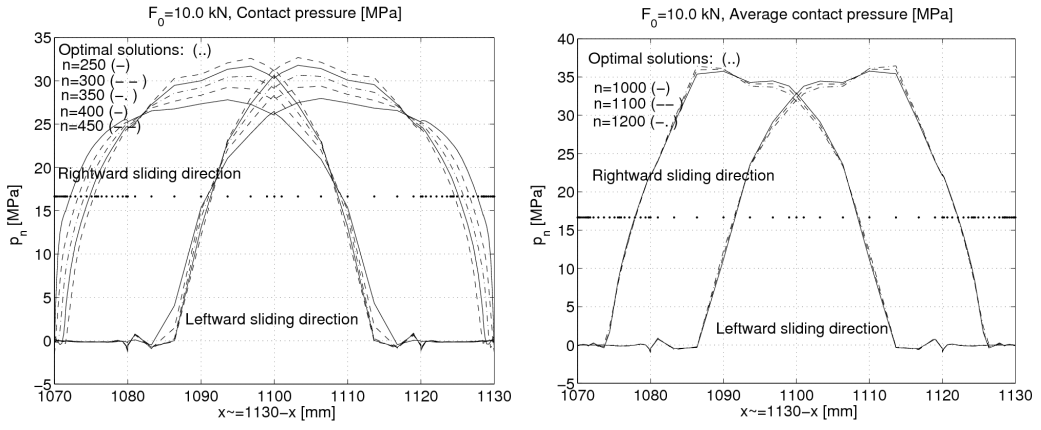

a) b)

Figure 11: Contact pressure at different time steps and sliding directions.

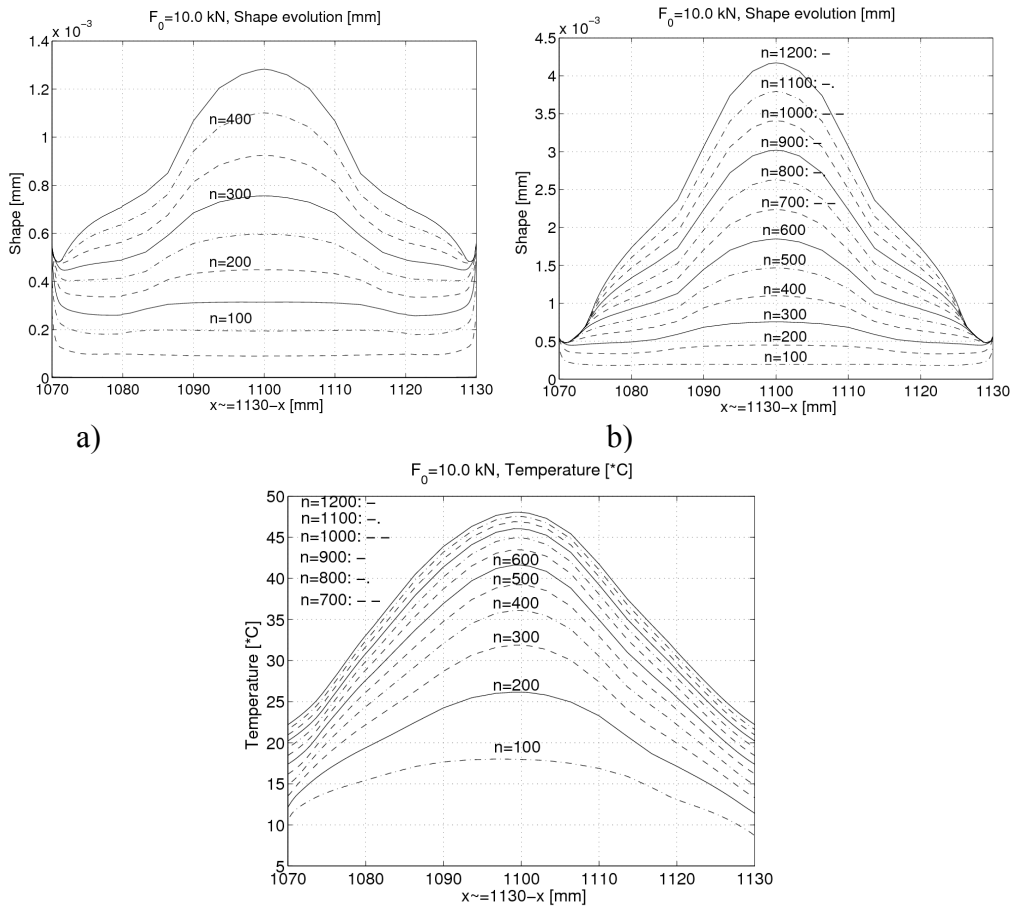

Figure 12: a) ,b) Evolution of shape of Body 1 at periodic motion of substrate in Figure 8 in the case of the heat generation, c) Temperature along the contact boundary in the punch at different time step

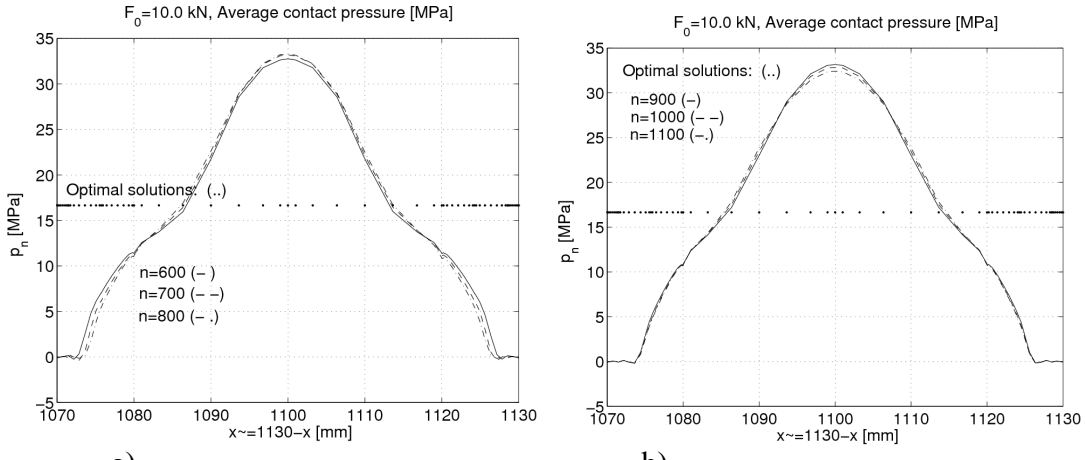

Figure 13: Average contact pressure of periodical motion at the different time step.

3 Concluding remarks

The recommended technique for solution of the coupled thermo-elastic-wear problem provides reasonable results for engineering applications The coupled thermo-mechanical problem is solved by operator split technique. The mechanical and thermal fields discretized by the finite element approximation are specified separately in the consecutive time steps.

The wear effect is calculated incrementally by applying the Archard type wear rule. The wear is accumulated at the end of half period of motion, so the contact pressure is fixed (at the iteration level), and the transient heat conduction problem is next solved for the given temperature field at the beginning of half period. The iterative process for one half period is terminated when the convergence criterion satisfies the error constraint for gap modification.

Numerical examples for different geometrical support conditions confirm the validity of prediction of the maximum value of temperature in the contact zone for the periodical motion of the strip. The results for the monotonic punch motion in the steady state wear state can be used to generate periodic solution.

Acknowledgement

The present research was partially supported by the Hungarian Academy of Sciences, by grant OTKA K67825, within the program TÁMOP 4.2.1.B-10/2/KONV-2010-0001 and by the Polish Ministry of Education and Science, Grant No.3 T08C 02129.

References

[1] I. Páczelt, Z. Mróz, “On optimal contact shapes generated by wear”, Int. J. Num. Meth. Eng., 63 , 1310-1347, 2005

[2] I. Páczelt, Z. Mróz, “On the analysis of steady sliding wear process”, Trib. Int., 42, 275-283, 2009.

[3] I. Páczelt, Z. Mróz, “Variational approach to the analysis of steady state thermo-elastic wear regimes”, Int. J. Num. Meth. Eng., 81, 728-760, 2010.

[4] Z. Mróz, I. Páczelt, “Analysis of thermo-elastic wear problems”, J. Thermal Stresses, 34-35, 569-606, 2011.

[5] I. Páczelt, Z. Mróz, “Numerical analysis of steady thermo-elastic wear regimes induced by translating and rotating punches”, Computes and Structures, 89, 2495-2521, 2011.

[6] I. Páczelt, Z. Mróz, “Solution of wear problems for monotonic and periodic sliding with p-version of the finite element method”, CMAME, 2012, to be accepted.

[7] U. Peigney, “Simulating wear under cyclic loading by a minimization approach”, Int. J. Solids and Structures 41, 6783-6799, 2004.

[8] N.H. Kim, D. Won, D. Burris, B. Holtkamp, G.C. Gessel, P. Swanson, W.G. Sawyer, "Finite element analysis and experiments of metal/metal wear in oscillatory contacts", Wear 258, 1787-1793, 2005.
[9] I.R. McColl, J. Ding, S.B. Leen, Finite element simulation and experimental validation of fretting wear, Wear 256, 1114–1127, 2004.
[10] I.G. Goryacheva, P.T. Rajeev, T.N. Farris, "Wear in partial slip contact", J. Tribology 123, 848-856, 2001.
[11] R. Komanduri, Z.B. Hou, "Analysis of heat partition and temperature distribution in sliding systems", Wear 251, 925-938, 2001.
[12] P. Zagrodzki, „Analysis of thermomechanical phenomena in mutidisc clutches and brakes", Wear 140, 291–308, 1990.
[13] K.J. Bathe, "Finite element procedures", Prentice Hall, Englewood Cliffs, New Jersy 07632, 1996.
[14] G. Zavarise, P. Wriggers, B. Schrefler, "On augmented Lagrangian algorithms for thermomechanical contact problems with friction", Int. J. Num. Meth. Eng. 38, 2929-2949, 1995.
[15] B. Szabó, I. Babuska, "Finite element analysis", Wiley-Intersience, New York, 1991.
[16] I. Páczelt, B. Szabó, T. Szabó, "Solution of contact problem using the hp-version of the finite element method", Comput. Math. Appl. 38, 49–69, 2000.